



# A New Infrared-Based Design for Measuring the Source to Skin Distance

## *Kaynak Cilt Mesafesi Ölçümüne Yönelik Kızılötesi Tabanlı Yeni Bir Tasarım*

Yalçın İşler<sup>1,2,\*</sup>, Alpman Manalp<sup>3,1,\*\*</sup>

<sup>1</sup>Izmir Katip Celebi University, Engineering and Architecture Faculty, Department of Biomedical Engineering, Cigli, Izmir, Turkey

<sup>2</sup>Islerya Medical and Information Technologies, Bornova, Izmir, Turkey

<sup>3</sup>Ege Oncology and Radiotherapy Center, 1428 Street, Kahramanlar, Izmir, Turkey

### Abstract

Cancer is a major public health problem worldwide. There are many types of cancer therapy methods including radiotherapy. In radiotherapy, positioning the patient to a consistent treatment location is significantly crucial to receive an effective dose, which closely affects the success of the therapy. The most commonly used parameter for ensuring the effective patient position is the source to skin distance (SSD). In this study, an infrared-based SSD measuring device is developed and its feasibility and accuracy are tested. The prototype of the infrared SSD measuring device (IRD) is composed of two major parts: a measuring distance sensor unit and a control unit. The microcontroller-based control unit displays the measurement in millimeters and transmits it to a computer via a serial port. The SSD measurement experiments were conducted on a Siemens Primus Linear Accelerator with a full-sized male phantom. Thirty measurements were conducted at different gantry angles for anatomic locations to determine the mean values and standard deviations. This device was tuned by a conventional mechanical ruler with an accuracy of 0.7324 mm. The results revealed that the proposed device gives more consistent and accurate readouts with smaller variations in all body functions than other devices.

**Keywords:** Linear accelerators, Patient setup, Positioning error, Source-to-skin distance

### Öz

Kanser dünya genelindeki başlıca toplum sağlığı sorunudur. Radyoterapi de dahil olmak üzere birçok kanser tedavi yöntemi bulunmaktadır. Radyoterapide sabit bir tedavi noktasına hastayı konumlandırmak tedavinin başarımını doğrudan etkileyen etkin doz alımı için oldukça önemlidir. Etkili hasta konumunu garanti altına almak için en çok kullanılan parametre kaynak cilt mesafesidir (SSD). Bu çalışmada, kızılötesi tabanlı bir SSD ölçüm cihazı geliştirilerek kullanılabilirliği ve doğruluğu test edilmiştir. Kızılötesi SSD ölçüm cihazının (IRD) örneği iki ana bileşenden oluşmaktadır: bir mesafe algılayıcısı ve bir kontrol birimi. Mikrodenetleyici tabanlı kontrol birimi ölçümü milimetre cinsinden ekranda gösterir ve seri port aracılığıyla bir bilgisayara aktarmaktadır. SSD ölçüm deneyleri gerçek boyutlu bir erkek model üzerinde Siemens Primus marka lineer algılayıcı ile gerçekleştirilmiştir. Farklı cihaz açıları ve anatomik konumların her biri için otuzar ölçüm alınarak ortalama ve standart sapmalar hesaplanmıştır. Cihaz geleneksel mekanik cetvel ile 0,7324 mm doğrulukta kalibre edilmiştir. Elde edilen sonuçlara göre, geliştirilen cihaz tüm vücut konumları için benzerlerinden daha düşük sapmalarla daha yüksek doğrulukta ölçüm sonuçları vermektedir.

**Anahtar Kelimeler:** Lineer hızlandırıcılar, Hasta düzeni, Konumlama hatası, Kaynak-cilt mesafesi

## 1. Introduction

Cancer is a major public health problem worldwide and is the second leading cause of death in the United States (Siegel et al. 2016). The estimated number of new cancer patients is 1,685,210 and the estimated number of death from cancer is 595,690 in the USA by 2016. In Korea, the

number of new cancer patients is 217,057 and the number of death from cancer is 76,611 by 2014 (Jung et al. 2017). For example, breast cancer is the most common cancer diagnosed among US women (excluding skin cancers) and is the second leading cause of cancer death among women after lung cancer (DeSantis et al. 2017).

There are many types of cancer therapy methods including but not limited to surgery, radiation therapy (or radiotherapy), chemotherapy, immunotherapy, targeted therapy, hormone therapy, stem cell transplant, and precision medicine

\*Corresponding author: [islerya@yahoo.com](mailto:islerya@yahoo.com)

Yalçın İşler [orcid.org/0000-0002-2150-4756](https://orcid.org/0000-0002-2150-4756)

Alpman Manalp [orcid.org/0000-0002-7006-6967](https://orcid.org/0000-0002-7006-6967)

(National Cancer Institute 2017). In addition to these methods, there are religious-based methods including yoga although evidence is insufficient to evaluate the efficacy of yoga in pediatric oncology (Danhauer et al. 2017). Besides, some patients will have only one treatment while most people have a combination of treatments, such as surgery with chemotherapy and/or radiation therapy (National Cancer Institute 2017).

Among these methods, radiation therapy (also called radiotherapy) uses high doses of radiation to kill cancer cells and to shrink tumors (National Cancer Institute 2018). In radiotherapy, positioning the patient to a consistent treatment location is significantly crucial to receive an effective dose. Miki et al studied 33 patients with pancreatic tumors. They emphasized that higher radiation dose must be limited to reduce the dose of organs at risk although it enhances the tumor control (Miki et al. 2017). A 3-mm of patient positioning error causes to decrease 38% dose in target tumors and to increase 41% dose in the surrounded spinal cord (Xing 2000). Liebl et al investigated dose distributions in photon radiotherapy (Liebl et al. 2014). They reported dose reductions of 50% in 2.8 mm and 90% in 7.2 mm for anatomy-based patient positioning. Kubota et al evaluated patient positioning based digital radiology imaging for 50 patients and reported that only 60% of positionings have acceptable accuracy (Kubota et al. 2018).

Quality assurance requires that the patient positioning error must be less than 3 mm but the desired error is less than 2 mm in radiotherapy (Foote et al. 2015). Nonetheless, setup errors between expected and actual fiducial points have been reported 5.8 mm for the supine position and 7.1 mm for the prone position by evaluating 83 patients with rectal cancer (Froseth et al. 2015). Patient positioning is an important issue even in veterinary applications (Hansen et al. 2015). In a recent study, imaging-based patient positioning has variations among decisions from five Finnish radiotherapy clinics (Siiskonen et al. 2017). Besides, patient discomforts should also be considered in positioning for favorable medical results (Boute et al 2018). Rehammar et al showed that radiotherapy for left-sided breast cancer is associated with a higher risk of heart disease than for right-sided with the largest increases seen in women who also received anthracycline-containing chemotherapy (Rehammar et al. 2017), which shows one of the side effects for radiotherapy and emphasizes the importance of accurate patient positioning.

The most commonly used parameter for ensuring the effective patient position is the source to skin distance

(SSD). SSD guarantees whether the patient is correctly positioned on the table as determined by the treatment plan. SSD is also used in verifying the depth of treatment for each external beam in clinical radiotherapy. The optical distance indicator (ODI), which is an embedded tool into medical linear accelerators (Linac), is the commercially-available device for this purpose (Maughan 1999). It projects a light through a mechanical image (ruler) onto the patient's skin. Since it is specifically designed as compatible with Linac, it has very common use in clinical radiotherapy. Nonetheless, there are many limitations in practice:

- Technicians may misread the distance.
- The body structure of the patient including the skin color and the roughness of the skin may influence the measurement.
- Illumination of the room may lead to misreading.
- The mechanical system may be affected by room temperature.
- As halogen lamps are used in the device, this also emits the heat and causes to decrease the life expectancy of other electronic components.
- Since filaments of lamps are so sensitive, these are broken down easily and treatment strategy may be delayed.
- Both installation and operational costs are high.

Although ODI is developed for self-diagnosis and calibration of the therapy machine, the mechanical front pointer (FP) has been used for this purpose, alternatively. A triangulation method based on a laser beam is announced for measuring SSD to be used in some specific clinical applications (Geyer 2003). This laser device was attached right next to the head of the Linac in the configuration. Alternatively, Us and Pepele reported that changes originated from SSD and gantry angle may be disregarded in dosimeters, but oblique beam projections in breast and head and neck patients should be taken into consideration (Us and Pepele 2017). In another study, an ultrasonic SSD measuring device (USD), which gives digital outputs simultaneously, is developed to eliminate the reading error caused by the misreading of visual projections on the patient's body (Feng et al. 2005). Nonetheless, almost all of these problems mentioned above are still present. Moreover, the therapy machine may clash the stretcher while the gantry of Linac is rotating around the stretcher. After all, these limitations make the measurement of SSD difficult (and occasionally impossible) and time-consuming process.

In addition to these devices, there are new emerging methods to quantify patient positioning. Padilla et al offered the use of MV portal films and skin markers together for whole-breast radiotherapy (Padilla et al. 2014). Kubota et al. (2015) developed a digital radiological imaging-based automatic evaluation system for prostatic cancers. Jia et al. (2015) used Kinect (gaming tool) for positioning and tracking radiotherapy patients. Heinz et al. (2016) developed a 3D registration based imaging to establish adequate patient positioning for stereotactic liver therapy patients. Walter et al. (2016) evaluated the positioning errors of a commercial 3D surface imaging system for radiotherapy patients. Gilles et al. (2016) used two cameras to obtain a more reliable patient positioning system. Ma et al. (2018) investigated an optical surface management system and cone-beam computed tomography for positioning over 200 patients with breast cancer. A recent method based on pressure distribution due to the patient's weight is patented (Ahn 2016). Another method based on determining patient position using the fluctuation of the electromagnetic field is patented (Birkenbach and Mangus 2018). Also, PET/CT imaging a potential tool for patient positioning in radiotherapy (Konert et al. 2015). Viergever et al. (2016) indicate the possibility of image registration of both 3D and 2D images in patient positioning.

In the current situation of daily clinical practice, new techniques for establishing adequate patient setup (specifically measuring the SSD) in radiation therapy are necessary because of increasing demand for using ultra-high-precise therapy devices. In this study, it is aimed to develop a new IRD to overcome these limitations listed above.

## 2. Materials and Method

The IRD is composed of two major parts: a distance measuring sensor unit and a microcontroller-based electronic control unit. These units are connected by a pair of cable.

### 2.1. Distance Measuring Sensor Unit

Sharp GP2Y0A02YK0F is a distance measuring sensor that is composed of an integrated combination of a position-sensitive detector, infrared emitting diode, and internal signal-processing circuitry. This unit outputs the analog voltage corresponding to the detection distance (Mustapha et al. 2013).

Because of the trigonometric structure of this type of sensors, the output is nonlinear with respect to the distance being measured (Figure 1) (Mustapha et al. 2013, Stanescu et al. 2014). There are three drawbacks noticed from this figure: (1) The output of the detector within the range of 20-150 cm is not linear, (2) the output of the detector within the range of less than 20 cm makes the measurement false, and (3) there are a few differences between distances measured with respect to the color of object.

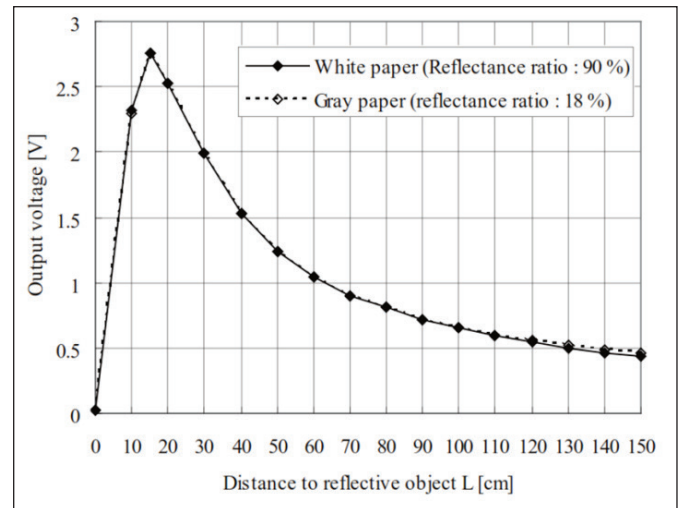


**Figure 1.** The output voltage to the distance characteristic curve of the distance measuring sensor unit (Sharp GP2Y0A02YK0F). The dashed line is related to grey paper with the reflectance ratio of 18% and the solid line is related to white paper with the reflectance ratio of 90%.

In order to overcome these drawbacks, there are some rules applied to the proposed design as described by (Acroname Robotoics 2013). The distance between source and skin is limited between 20 and 150 cm to avoid misinterpretation area. Next, the measured voltage is normalized by using a look-up table.

- This sensor was selected due to the following advantages (Mustapha et al. 2013, Stanescu et al. 2014):
- There are only a few voltage differences between white and black objects (Figure 1).
- It needs 4.5 to 5.5 volts, which is easy to supply.
- The variety of reflectivity of the object is not influenced.
- The environmental temperature is not influenced.
- The operation duration is not influenced.
- The cost of the sensor is less than \$15.

## 2.2. Control Unit

A microcontroller board using the PIC18F452 microcontroller, which is a low-cost general-purpose 8-bit microcontroller, is developed. This microcontroller has eight analog-to-digital converters (ADCs), 8192 bytes read-only program memory (ROM), 384 bytes general-purpose memory (RAM), integrated communication hardware for both serial and two-wire (I2C), and maximum clock frequency of 40 MHz (which determines the speed of the system) (Microchip 1997). Additional quad 7-segment display and TTL-RS232 serial converter integrated circuits have been embedded with the microcontroller in a single electronic board (Fig. 2). Each display is combined with a 74HC595 serial-in-parallel-out latch integrated circuit to store the number to be displayed. Displays are used to show the distance in millimeters. Unused pins of the microcontroller are connected to empty slots on the board for further developments. The cost of the control unit, including printing and soldering the board, is less than \$24.

## 2.3. Software

CCS C compiler version 4.128 was used to implement all algorithms into the single microcontroller (Cicek 2012). While the control unit is running, it shows the measured distance on 7-segment displays and transmits the value to the PC or another device via serial port at the same time.

All sensor measurements were digitized by 10-bit internal ADC, which means  $\pm 0.7324$  mm ( cm) sensitivity for each measurement.

In addition, median filtering was used to prevent noises. The distance was obtained by the median value of the successive five readings. After obtaining the analog value, the corresponding distance was found by using a look-up table embedded into the EEPROM memory of the microcontroller.

## 2.4. Implementation

First, all the design was tested using the simulation software

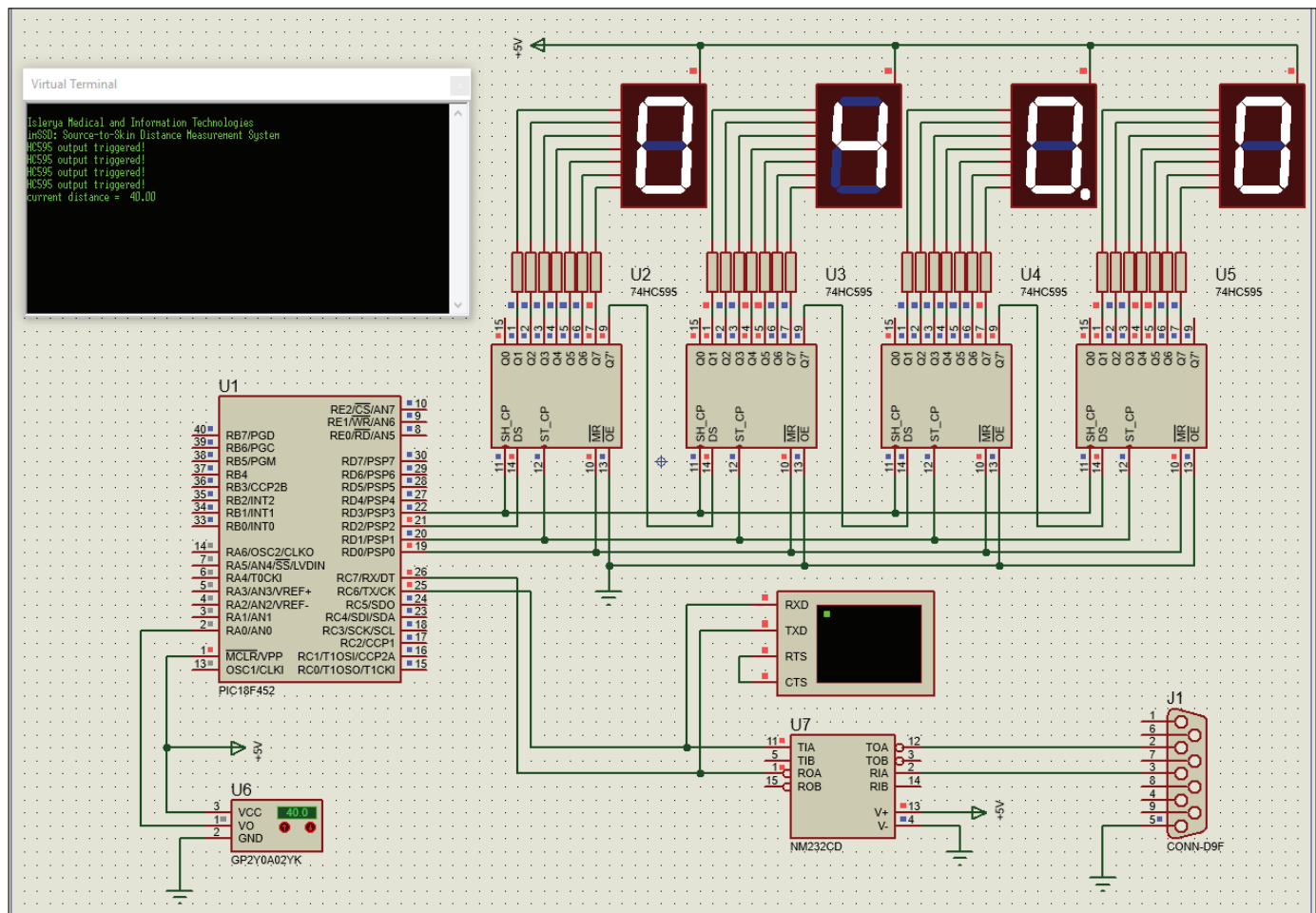


Figure 2. Electronic schematics of the control unit while the simulation is running. Example measurement is seen as 40.0 centimeters.

of Proteus version 8.1 (Labcenter Electronics 2015). The final simulated system has been implemented with a 1521-lines source code file and 3682 bytes program memory in the microcontroller.

### 2.5. One-Sample T-Test

This statistical test determines whether the measurements obtained from the proposed system is statistically different from a predetermined measurement acquired using a mechanical ruler since it has been accepted as a gold standard in SSD measurement literature. This test requires the following conditions (Akgul 2003):

- Test variable must be continuous,
- Measurements (observations) are independent,
- Normal (at least similar) distribution is required on the observations,
- The normality can be neglected if the number of samples is large enough ( $\geq 30$  thanks to the central limit theorem (Fischer 2011)),
- Outliers should be excluded from the observations.

The t statistic is calculated as

$$t = \frac{\bar{xx} - \mu}{s_{xx}} \quad (1a)$$

where

$$s_{xx} = \frac{s}{\sqrt{n}} \quad (1b)$$

Here  $\mu$  is the predetermined constant,  $\bar{xx}$  is the sample mean,  $n$  is the number of observations,  $s$  is the standard deviation, and  $s_{xx}$  is the estimated standard error of the observations. Then, this value of  $t$  is compared to a critical value from the  $t$  distribution table with degrees of freedom ( $df=n-1$ ) and chosen confidence level ( $\alpha=0.05$ ). If the calculated  $t$  value is less than the critical  $t$  value, then we can reject the null hypothesis (Akgul 2003).

### 3. Results and Discussion

Experiments on measuring SSD were conducted by using the prototype IRD on a therapy device of Siemens Primus Linac with the application with a full-sized male phantom by following the same procedure described in (Feng et al 2005). The measurements of SSD were acquired from different body parts of the phantom (head, thorax, breast, and pelvis). The same measures were recorded by both a mechanical ruler and the proposed design at different gantry angles. The mechanical ruler was already mounted on the

therapy device before the experiments. Each measure was repeated 30 times at each gantry angle for all anatomic parts as noted above. Then, the mean values and the standard deviations were calculated as

$$LL = \frac{\sum |L_i|}{N} \quad (2a)$$

and

$$SD = \sqrt{\frac{(L_i - LL)^2}{N-1}} \quad (2b)$$

where  $LL$  is the mean value,  $SD$  is the standard deviation,  $N$  is the number of measurement,  $L_i$  is  $i$ -th measurement.

As a result, 240 measurements were recorded during this study and summarized in Table 1. In each body location, the measurement errors are less than 0.3 mm where the average of absolute errors is less than 0.1 mm and the standard deviation is less than 0.4 mm.

The statistical difference between measurements and the measurement from the mechanical ruler is calculated by using the one-sample t-test in the version 24 of SPSS software (possibly the most commonly used software on statistics). Since all  $p$  values are greater than 0.05 (our statistical significance level) in Table 1, we accept that all measurements from the proposed IRD device belong to the gold standard of the mechanical ruler, which shows that there is no significant statistical difference.

The mean values of standard deviations calculated from all measurements were compared to that of other methods in Table 2. These results indicate that the minimum variation can be achieved in the proposed method, which means that IRD gives the most repeatable and reliable digital readouts for measuring SSD among other methods reported in the literature.

The total cost of all the materials used in the hardware is less than \$24 (Table 3). This is a very low cost when compared to the cost of the USD alternative of \$3,000 (Feng et al 2005), which is the minimum cost among other SSD measurement methods.

Since the radiation oncology progresses toward more precise intensity-modulated radiation therapy techniques, setup errors become substantially important. Hence, the accurate measurement of a patient to the radiation source in radiotherapy is crucial to give correct doses to the patient. Therefore, a number of different tools for positioning the patient have also been developed. Most of the other SSD measurement devices are negatively affected by several

**Table 1.** SSD measurements at different body locations made with a commercial mechanical ruler and the proposed design. LL is the Mean Value, SD is Standard Deviation, SSD is Source to Skin Distance, IRD is Proposed Infrared SSD Measurement Device. P-value gives the statistical significance value calculated by the One-Sample T-Test. If p-value higher than a threshold (0.05), then this measurement doesn't show a statistically significant difference between the proposed IRD method and the mechanical ruler of the gold standard.

Field Location	Gantry Angle (o)	Mechanical Ruler (mm)	IRD LL $\pm$ SD (mm)	p-value
Head	0	800.5	800.62 $\pm$ 0.28	0.18
Head	90	789.3	789.26 $\pm$ 0.17	0.48
Thorax	0	802.2	802.03 $\pm$ 0.15	0.20
Thorax	90	785.1	784.96 $\pm$ 0.30	0.19
Breast	45	910.0	909.56 $\pm$ 0.40	0.11
Breast	-45	920.1	920.15 $\pm$ 0.39	0.73
Pelvis	0	860.0	860.06 $\pm$ 0.17	0.35
Pelvis	90	810.2	810.15 $\pm$ 0.22	0.52

**Table 2.** Measurement errors calculated from all SSD measurements made with all known devices given in the literature and proposed device. All values are given as Mean  $\pm$  Standard Deviation (SD) where SD is available.

Method	Measurement Error Mean $\pm$ SD (mm)	Note
Portal MV Imaging (Padilla et al 2014)	9.40 $\pm$ 4.00	Breast only
Optical Distance Indicator (ODI) (Maughan 1999)	2.80	Whole body
Infrared Based Device (Kinect) (Jia et al 2015)	2.00 $\pm$ 0.03	Whole body
Front Pointer (FP) (Geyer 2003)	1.66	Whole body
Optical Surface Scanning (Catalyst) (Walter et al 2016)	1.41 $\pm$ 3.56	Whole body
Two Time-of-Flight Cameras (ToF) (Gilles et al 2016)	0.80 $\pm$ 0.70	Whole body
Cone-Beam Computed Tomography (CBCT) (Walter et al 2016)	0.70 $\pm$ 2.37	Whole body
Ultrasonic Device (USD) (Feng et al 2005)	0.55	Whole body
3-D Registration (Heinz et al 2016)	0.50 $\pm$ 0.28	Whole body
Cone-Beam Computed Tomography (CBCT) (Ma et al 2018)	0.45 $\pm$ 2.42	Breast only
Optical Surface Management System (OSMS) (Ma et al 2018)	0.41 $\pm$ 2.56	Breast only
Digital Radiology System (Kubota et al 2015)	0.32 $\pm$ 0.18	Prostate only
<b>Proposed Infrared-Based Device (IRD)</b>	<b>0.08 <math>\pm</math> 0.32</b>	<b>Whole body</b>

**Table 3.** Bill of materials for the proposed study.

Components	Unit Price (US \$)	Quantity	Price (US \$)
PIC18F452	2.78	1	2.78
LCD 2x16	2.16	1	2.16
PCB	3.87	1	3.87
GP2Y0A02YK0F	14.07	1	14.07
MAX232C	0.37	1	0.37
D-Sub Connector	0.25	1	0.25
LM324 Op. Amp.	0.11	1	0.11
Resistors	0.01	16	0.16
Capacitors	0.01	4	0.04
<b>Total</b>			<b>23.81</b>

environmental factors including room temperature and the color of the patient's skin. The proposed infrared-based device seems to be a great candidate to eliminate many of these issues.

The IRD has several advantages. First, the infrared sensor can be mounted inside or near the block tray of the therapy device so that it can be placed right next to the radiation beam, which helps to acquire more precise SSD measures. This also results in shortening the patient-setup time due to no blockage of the device by the patient or by the immobilization of the device. Second, the IRD method gives the most accurate measures among other methods reported in the literature. Third, the digital displays prevent the possible human errors relevant to a misreading of visual scales, especially in improper positions. Finally, many environmental factors including the room temperature, reflectivity of the subject, and the skin color of the patient do not affect the SSD measurement.

Using the proposed SSD measurement device, the quality of treatment can be improved while risks of applying over or under dose are prevented since IRD gives the minimum standard deviation (which means maximum repeatability) in SSD measurements.

Besides the benefits of the proposed design, IRD is also very competitive by its cost. Overall, we believe that the IRD is a handy, effortless, speedy and truthfully alternative for obtaining the SSD. Further improvements regarding the integration of SSD into the Linac head and clinical validation should be studied in the future.

#### 4. References

- Acroname Robotics. 2013.** *Linearizing Sharp Ranger Data.* <https://acroname.com/articles/linearizing-sharp-ranger-data>
- Ahn, PHK. 2016.** Patient positioning system and methods for diagnostic radiology and radiotherapy. *United States Patent Office* US 9433387, 6 September 2016.
- Akgul, A. 2003.** *Statistical Analysis Techniques in Medical Researches: SPSS Experiments.* Ankara: Seckin Yayıncılık, Turkey, (in Turkish).
- Birkenbach, R., Manus, J. 2018.** Patient positioning system with an electromagnetic field generator of an electromagnetic tracking system. *United States Patent Office* US 9918797, 20 March 2018.
- Boute, B., Veldeman, L., Speleers, B., Van Greveling, A., Van Hoof, T., Van de Velde, J., Vercauteren, T., De Neve, W., Detand, J. 2018.** The relation between patient discomfort and uncompensated forces of a patient support device for breast and regional lymph node radiotherapy. *Appl. Ergon.*, 72: 48-57.
- Cicek, S. 2012.** *CCS C and PIC Programming*, (7th ed.). Altas Publishing, Turkey, (in Turkish).
- Danhauer, SC., Addington, EL., Sohl, SJ., Chaoul, A., Cohen, L. 2017.** Review of yoga therapy during cancer treatment. *Support Care Cancer* 25(4): 1357-1372.
- DeSantis, CE., Ma, J., Sauer, AG., Newman, LA., Jemal, A. 2017.** Breast cancer statistics 2017: racial disparity in mortality by state. *CA Cancer J. Clin.*, 67(6): 439-448.
- Feng, Y., Allison, R., Hu, XH., Mota, H., Jenkins, T., Wolfe, M.L., Sibata, C. 2005.** An ultrasonic device for source to skin distance measurement in patient setup. *Int. J. Radiation Oncology Biol. Phys.*, 61(5): 1587-1589.
- Fischer, H. 2011.** *A History of the Central Limit Theorem: From Classical to Modern Probability Theory.* Springer-Verlag New York Inc, New York, NY, United States.
- Foot, M., Bailey, M., Smith, L., Siva, S., Hegi-Johnson, F., Seeley, A., Barry, T., Booth, J., Ball, D., Thwaites, D. 2015.** Guidelines for safe practice of stereotactic body (ablative) radiation therapy. *J. Med. Imag. Radiat. On.*, 59: 646-653.
- Froeth, TC., Strickert, T., Solli, KS., Salvesen, O., Frykholm, G., Reidunsdatter, RJ. 2015.** A randomized study of the effect of patient positioning on setup reproducibility and dose distribution to organs at risk in radiotherapy of rectal cancer patients. *Radiat. Oncol.*, 10: 217.1-9.
- Geyer, R. 2003.** Source-skin-distance measurements using an off-axis laser device. *Med. Phys.*, 30: 1436.
- Gilles, M., Fayad, H., Migliorini, P., Clement, J.F., Scheib, S., Cozzi, L., Bert, J., Boussion, N., Schick, U., Pradier, O., Visvikis, D. 2016.** Patient positioning in radiotherapy based on surface imaging using time of flight cameras. *Med. Phys.*, 43(8): 4833-4841.
- Hansen, KS., Theon, AP., Dieterich, S., Kent, MS. 2015.** Validation of an indexed radiotherapy head positioning device for use in dogs and cats. *Vet. Radiol. Ultrasound.* 56(4): 448-455.
- Heinz, C., Gerum, S., Freislederer, P., Ganswindt, U., Roeder, F., Corradini, S., Belka, C., and Niyazi, M. 2016.** Feasibility study on image guided patient positioning for stereotactic body radiation therapy of liver malignancies guided by liver motion. *Radiat. Oncol.*, 11: 88.1-7.
- Jia, J., Xu, G., Pei, X., Cao, R., Hu, L., Wu, Y. 2015.** Accuracy and efficiency of an infrared based positioning and tracking system for patient set-up and monitoring in image guided radiotherapy. *Infrared Phys. Technol.*, 69: 26-31.

- Jung, KW., Won, YJ., Kong, H.J., Lee, ES. 2018.** Cancer statistics in Korea: incidence, mortality, survival, and prevalence in 2015. *Cancer Res. Treat.*, 49(2): 292-305.
- Konert, T., Vogel, W., MacManus, MP., Nestle, U., Belderbos, J., Gregoire V., Thorwarth, D., Fidarova, E., Paez, D., Chiti, A., Hanna, GG. 2015.** PET/CT imaging for target volume delineation in curative intent radiotherapy of non-small cell lung cancer: IAEA consensus report 2014. *Radiother Oncol.*, 116: 27-34.
- Kubota, Y., Tashiro, M., Shinohara, A., Abe, S., Souda, S., Okada, R., Ishii, T., Kanai, T., Ohno, T., and Nakano, T. 2015.** Development of an automatic evaluation method for patient positioning error. *J. Appl. Clin. Med. Phys.*, 16(4): 100-111.
- Kubota, Y., Hayashi, H., Abe, S., Souda, S., Okada, R., Ishii, T., Tashiro, M., Torikoshi, M., Kanai, T., Ohno, T., and Nakano, T. 2018.** Evaluation of the accuracy and clinical practicality of a calculation system for patient positional displacement in carbon ion radiotherapy at five sites. *J. Appl. Clin. Med. Phys.*, 19(2): 144-153.
- Labcenter Electronics. 2015.** *Proteus Design Suite*.
- Liebl, J., Paganetti, H., Zhu, M., Winey, BA. 2014.** The influence of patient positioning uncertainties in proton radiotherapy on photon range and dose distributions. *Med. Phys.*, 41(9): 091711.1-12.
- Ma, Z., Zhang, W., Su, Y., Liu, P., Pan, Y., Zhang, G., Song, Y. 2018.** Optical surface management system for patient positioning in interfractional breast cancer radiotherapy. *Biomed. Res. Int.*, 6415497.1-8.
- Maughan, RL. 1999.** Designing an optical distance indicator for a radiation therapy accelerator. *Med. Phys.*, 26: 236-238.
- Microchip. 1997.** *PIC Micro Mid-Range MCU Family Reference Manual*. Microchip USA: Microchip Technology Incorporated.
- Miki, K., Fukahori, M., Kumagai, M., Yamada, S., Mori, S. 2017.** Effect of patient positioning on carbon-ion therapy planned dose distribution to pancreatic cancer tumors and organs at risk. *Physica Med.*, 33: 38-46.
- Mustapha, B., Zayegh, A., Begg, RK. 2013.** Ultrasonic and infrared sensors performance in a wireless obstacle detection system. *2013 1st International Conference on Artificial Intelligence, Modelling and Simulation (AIMS)* Kota Kinabalu, Malaysia, 3-5 December 2013.
- National Cancer Institute. 2017.** *Types of Cancer Treatment*, <https://www.cancer.gov/about-cancer/treatment/types>, last updated April 6, 2017 and last visited February 13, 2019.
- National Cancer Institute. 2018.** *Radiation Therapy to Treat Cancer*, <https://www.cancer.gov/about-cancer/treatment/types/radiation-therapy>, last reviewed May 1, 2018, and last visited February 13, 2019.
- Padilla, L., Kang, H., Washington, M., Hasan, Y., Chmura, S., Al-Hallaq, H. 2014.** Assessment of interfractional variation of the breast surface following conventional patient positioning for whole-breast radiotherapy. *J. Appl. Clin. Med. Phys.*, 15(5): 177-189.
- Rehammar, JC., Jensen, MB., McGale, P., Lorenzen, EL., Taylor, C., Darby, SC., Videbaek, L., Wang, Z., Ewertza, M. 2017.** Risk of heart disease in relation to radiotherapy and chemotherapy with anthracyclines among 19464 breast cancer patients in Denmark 1977-2005. *Radiother Oncol.*, 123(2): 299-305.
- Siegel, RL., Miller, K.D., Jemal, A. 2016.** Cancer statistics 2016. *CA. Cancer J. Clin.*, 66(1): 7-30.
- Siiskonen, T., Kajjaluo, S., Florea, T. 2017.** Imaging practices and radiation doses from imaging in radiotherapy. *Physica Med.* 42: 247-252.
- Stanescu, T., Dolg, V., Mondoc, A. 2014.** Random issues in workspace analysis for a mobile robot. *AIP Conf Proc* 1637(1): 1254.
- Us, B., Pepele, EK. 2017.** An experimental study on the determination of gantry angle and SSD dependencies of TLD and MOSFET dosimeter systems. *Int. J. Radiat. Res.*, 15(1): 117-121.
- Viergever, MA., Maintz, JBA., Klein, S., Murphy, K., Staring, M., Pluim, JPW. 2016.** A survey of medical image registration. *Med. Image Anal.*, 33: 140-144.
- Walter, F., Freislederer, P., Belka, C., Heinz, C., Sohn, M., Roeder, F. 2016.** Evaluation of daily patient positioning for radiotherapy with a commercial 3D surface-imaging system (Catalyst). *Radiat. Oncol.*, 11: 154.1-8.
- Xing, L. 2000.** Dosimetric effects of patient displacement and collimator and gantry angle misalignment on intensity modulated radiation therapy. *Radiat. Oncol.*, 56(1): 97-108.